

# Increased Calcium Influx in Dystrophic Muscle

Paul R. Turner, Peking Fong, Wilfred F. Denetclaw, and Richard A. Steinhardt

Department of Molecular and Cell Biology, Division of Cell and Developmental Biology, University of California, Berkeley, California 94720

**Abstract.** We examined pathways which might result in the elevated resting free calcium ( $[Ca^{2+}]_i$ ) levels observed in dystrophic mouse (*mdx*) skeletal muscle fibers and myotubes and human Duchenne muscular dystrophy myotubes. We found that *mdx* fibers, loaded with the calcium indicator fura-2, were less able to regulate  $[Ca^{2+}]_i$  levels in the region near the sarcolemma. Increased calcium influx or decreased efflux could lead to elevated  $[Ca^{2+}]_i$  levels. Calcium transient decay times were identical in normal and *mdx* fibers if resting  $[Ca^{2+}]_i$  levels were similar, suggesting that calcium-sequestering mechanisms are not altered in dystrophic muscle, but are slowed by the higher resting  $[Ca^{2+}]_i$ . The defect appears to be specific for calcium since resting free sodium levels and sodium in-

flux rates in the absence of  $Na^+/K^+$ -ATPase activity were identical in normal and dystrophic cells when measured with sodium-binding benzofuran isophthalate. Calcium leak channels, whose opening probabilities ( $P_o$ ) were voltage independent, could be the major calcium influx pathway at rest. We have shown previously that calcium leak channel  $P_o$  is significantly higher in dystrophic myotubes. These leak channels were selective for calcium over sodium under physiological conditions. Agents that increased leak channel activity also increased  $[Ca^{2+}]_i$  in fibers and myotubes. These results suggest that increased calcium influx, as a result of increased leak channel activity, could result in the elevated  $[Ca^{2+}]_i$  in dystrophic muscle.

THE gene product missing in Duchenne muscular dystrophy (DMD)<sup>1</sup> is dystrophin (Hoffman et al., 1987a,b), a 400-kD protein which subsequently has been localized to the sarcolemma of skeletal muscle (Sugita et al., 1987; Zubrzycka-Gaarn et al., 1988). In the dystrophic mouse (*mdx*), muscle degeneration begins shortly after birth as a result of a mutation of the X chromosome (Bulfield et al., 1984). As in the human, this mutation results in a lack of dystrophin expression in muscle (Hoffman et al., 1987a,b). Dystrophin has some sequence homology with cytoskeletal proteins and binds to several integral membrane glycoproteins (Campbell and Kahl, 1989; Ohlendieck et al., 1991), but the function of dystrophin remains unknown.

The location of dystrophin, and the finding that the total calcium content of dystrophic muscle is increased early in the disease (Bertorini et al., 1982), support a theory of altered calcium ion regulation in DMD, perhaps as the result of a defective sarcolemma (Duncan, 1978). Further support for this theory has come from studies showing that resting intracellular free calcium ( $[Ca^{2+}]_i$ ) levels are elevated in *mdx* muscle fibers (Turner et al., 1988; Williams et al., 1990) and in cultured dystrophic human and mouse muscle

(Mongini et al., 1988; Fong et al., 1990). An increase in muscle protein degradation is directly related to this elevated  $[Ca^{2+}]_i$  in the *mdx* mouse (Turner et al., 1988; MacLennan et al., 1991). In this paper, we further examined the impaired calcium ion homeostasis in dystrophic muscle by looking for regional differences in  $[Ca^{2+}]_i$  in normal and dystrophic fibers and myotubes, using the fluorescent calcium indicator, fura-2.

The elevated  $[Ca^{2+}]_i$  in dystrophic muscle could be a result of increased calcium ion influx or reduced calcium efflux. Calcium transients, resulting from electrical depolarization, are prolonged in *mdx* fibers (Turner et al., 1988). This suggests that mechanisms for sequestering calcium may be impaired in dystrophic muscle (Duncan, 1978). Alternatively, calcium sequestration rates could be slowed as a result of the elevated resting  $[Ca^{2+}]_i$  levels in dystrophic muscle. Since  $[Ca^{2+}]_i$  can be manipulated by varying extracellular free calcium concentration ( $[Ca^{2+}]_o$ ) (Turner et al., 1988), we recorded calcium transients in *mdx* fibers before and after resting  $[Ca^{2+}]_i$  levels were lowered to normal levels. We also recorded transients in normal fibers before and after raising  $[Ca^{2+}]_i$  to *mdx* levels.

Increased calcium influx into dystrophic muscle could result from a nonspecific permeability increase of the sarcolemma to all cations. Such an increase could also result in elevated resting intracellular free sodium ion concentrations ( $[Na^+]_i$ ) in dystrophic cells. We therefore measured both resting  $[Na^+]_i$  levels and sodium influx rates in normal and

1. *Abbreviations used in this paper:* AM-ester, acetoxymethyl ester;  $[Ca^{2+}]_i$ , intracellular free calcium concentration;  $[Ca^{2+}]_o$ , extracellular free calcium concentration; DMD, Duchenne muscular dystrophy;  $E_{rev}$ , potential at which channel current reverses direction; *fdb*, *flexor digitorum brevis*;  $[Na^+]_i$ , intracellular free sodium ion concentration;  $P_o$ , opening probability; SBFI, sodium-binding benzofuran isophthalate.

dystrophic cells using sodium-binding benzofuran isophthalate (SBFI), a fluorescent sodium indicator (Minta and Tsien, 1989).

We have reported previously that a class of leak channels, permeable to both barium and calcium, are open more frequently in dystrophic mouse and human myotubes (Fong et al., 1990). If leak channels are a major pathway for increased calcium entry into dystrophic cells at rest, the opening of these channels should be voltage independent. The permeability of the leak channel to calcium in the presence of physiological sodium levels was examined. If calcium influx via leak channels contributes to resting  $[Ca^{2+}]_i$  levels, then altered leak channel activity should result in altered  $[Ca^{2+}]_i$  levels. We therefore examined the effects of various agents on leak channel opening probability ( $P_o$ ) and also tested their effect on  $[Ca^{2+}]_i$  levels in myotubes and fibers.

## Materials and Methods

### Cells

Skeletal muscle fibers from the *flexor digitorum brevis* (*fdb*) were dissected intact from the hind feet of normal and *mdx* mice aged 3–6 wk. The muscle tendons were pinned at resting lengths to a silicon circle on a glass-bottomed petri dish. Initial sarcomere lengths were  $\sim 2.0 \mu\text{M}$ . We used a Ringer's solution containing (mM) NaCl, 138; KCl, 2.7;  $CaCl_2$ , 1.8;  $MgCl_2$ , 1.06; glucose, 5.6; and Na-Hepes, 12.4, pH 7.20. Primary mouse myoblasts were obtained from hind limb muscles (Dimario and Strohmman, 1988), and human clonal myoblasts were from frozen stocks (Fong et al., 1990). After differentiation in DME with 10% horse serum, mouse myotubes were present at day 2, and human myotubes at day 4. Culture medium was replaced with Ringer's before all experiments.

### Free Calcium Measurements

Fibers and myotubes were loaded with the calcium-sensitive dyes fura-2 and fluo-3 (Molecular Probes, Inc., Eugene, OR) by hydrolysis of their acetoxymethyl (AM) esters. A 10-mM dye stock in DMSO was mixed with an equal volume of Pluronic F-127 (Molecular Probes, Inc.) before dilution to a final concentration of 1  $\mu\text{M}$  fura-2 or 2  $\mu\text{M}$  fluo-3. Cells were loaded for 30–60 min at 25°C. Measurements at 25°C were made for up to  $\sim 1$  h after loading and for shorter periods at 37°C, since dye loss and/or compartmentation occurred more rapidly at this temperature (Poenie et al., 1985). Calibration of fura-2 signals was as described previously; free calcium was calculated from the fluorescence ratio obtained by dividing the fluorescence (520-nm) values from excitation at 350 nm by those at 385 nm (Grynkiewicz et al., 1985; Turner et al., 1988). For fluo-3 measurements, a 490-nm excitation filter was used. Fluo-3 was calibrated by adding 1  $\mu\text{M}$  ionomycin (Calbiochem Corp., La Jolla, CA) in the presence of saturating  $[Ca^{2+}]_o$ ; subsequently the signal was quenched by addition of 2 mM  $MnCl_2$ . Cells were lysed with 140  $\mu\text{M}$  digitonin (Fisher Scientific, Fair Lawn, NJ) to obtain the cell backgrounds (Kao et al., 1989).

### Imaging

An inverted microscope (model IM-35, Carl Zeiss, Inc., Thornwood, NY) set up for epifluorescence was modified for fluorescence ratio imaging as described in Poenie et al. (1985). Fluorescence ratios of fura-2-loaded myotubes and adult mouse fibers were detected using a Dage 66 Silicon Intensified Target camera (Dage-MTI Inc., Michigan City, IN) and digitized with an image processor (model 5000; Gould Inc., Glen Burnie, MD) under the control of PDP 11/73 microcomputer (Digital Equipment Corp., Marlboro, MA). The resulting images were stored for analysis on a Panasonic optical laser disk. All experiments were performed at 37°C and ratio images were taken at intervals for, at most, up to  $\sim 60$  min after loading.

### Calcium Transient Recording

Repetitive depolarizing pulses from a Grass stimulator (model SD5; Grass Instr. Co., Quincy, MA) were sent to platinum electrodes, placed on each

side of a pinned muscle fiber which had been loaded with dye (fura-2 or fluo-3). Average dye concentrations in fibers after this loading procedure were 25–30  $\mu\text{M}$ . Transients in fibers loaded with 5–10  $\mu\text{M}$  dye were not different in amplitude or kinetics compared with those in fibers loaded with 40–50  $\mu\text{M}$  dye. However, transient records from lightly loaded fibers had more scatter. Stimulating frequency was usually 3.3 Hz. Data collection began 100  $\mu\text{s}$  after each stimulus. Stimulation and data collection were computerized (data acquisition software by Chester M. Regan, University of Illinois, Champaign-Urbana, IL). A slit aperture excluded fluorescence from adjacent fibers. Extra care had to be taken with fluo-3-loaded fibers to avoid movement artifacts. The slit aperture was positioned over the fiber, and stimulating electrodes placed on both sides near the center of the fiber. The fiber, which was stretched to approximately normal resting length, was initially examined with visible light to ensure that the fiber was not moving out of the optical path when stimulated. If any movement artifacts in the record were observed, such as a rapid drop in signal intensity followed by recovery, the fiber, electrodes or slit aperture, were repositioned, and the trial repeated.

At least 10 transients were averaged at each wavelength. The data was collected in 100- $\mu\text{s}$  bins, before division by the computer to produce a ratio record of the transients. Noise in a record could be reduced by averaging a larger number of transients or by increasing the data bin size. However, the latter option was not tried since it would reduce the temporal resolution. The decay half time ( $t_{1/2}$ ) was determined graphically from each record as the duration in which the response dropped by 50% from the peak towards the "steady-state" level at the end of the 100-ms sampling period.

### Sodium Measurements

The fluorescent sodium dye SBFI (Molecular Probes, Inc.) was loaded into fibers by microinjection (for method see Turner et al., 1986) and into fibers and myotubes by hydrolysis of the membrane-permeant AM-ester. A 10-mM SBFI (potassium salt) stock in 10 mM K-Hepes, pH 7.2, was microinjected into fibers ( $\sim 0.5\%$  cell volume). SBFI-AM was loaded by incubation for 1 h at 25°C. A 10-mM stock in DMSO was mixed with an equal volume of 25% wt/vol Pluronic before dilution in Ringer's to a final concentration of 2  $\mu\text{M}$  SBFI. Measurements were performed up to  $\sim 1$  h after dye loading to minimize possible compartmentation. Calibrations were made *in vivo* by addition of a 1:1 monensin and nigericin stock (Calbiochem Corp.) to a final concentration of 2  $\mu\text{M}$  in a Ringer's which contained 110 mM Na gluconate, 30 mM NaCl, 1.8 mM  $CaCl_2$ , 1.0 mM  $MgCl_2$ , 2.3 mM KCl, and 12 mM Na-Hepes, pH 7.2. This was followed by several changes of extracellular free sodium concentration ( $[Na^+]_o$ ) (Harootyan et al., 1989).

Resting  $[Na^+]_i$  levels were also measured with liquid ion exchanger electrodes made according to the method of Tsien and Rink (1980) using prepared solution 71176 (Fluka Chem. Corp., Ronkonkoma, NY).

### Patch Clamp Techniques

Single channels in cultured myotubes were measured using conventional patch clamp techniques (Hamill et al., 1981). Electrodes were fire polished to resistances of 5–13 M $\Omega$ , and coated with Sylgard (Dow Corning Corp., Midland, MI). Cell-attached patches were formed using slight positive pressure to prevent adherence to the pipette tip of any seal-discouraging particles while approaching the cell, followed by gentle suction on contact. Seal resistances were 1–30 G $\Omega$ . Inside-out excised patches were formed by gently pulling the pipette away from the cell surface; the pipette tip was only infrequently passed through the air-water interface (Hamill et al., 1981). Data was acquired using an Axopatch 1-C amplifier (Axon Instruments, Inc., Burlingame, CA) interfaced to an IBM AT-compatible computer with a Tecmar DA/AD board (Scientific Solutions, Solon, OH) and filtered at two kHz using a -3 dB, four-pole Bessel low-pass filter. Sampling rate was 40–100  $\mu\text{s}$  for these records, which were acquired using the Fetchex routine of pClamp (Axon Instruments, Inc.). We also used the Axotape acquisition program (Axon Instruments, Inc.) for longer recording sessions. These data were sampled at  $\sim 700 \mu\text{s}$  ( $\sim 1.5$  kHz) and filtered at 0.5 or 1 kHz before analysis using pClamp. The standard pipette filling solution consisted of 96 mM  $BaCl_2$ , 12.4 mM Hepes, pH 7.2 (titrated with  $BaOH_2$ ). To minimize spontaneous myotube contractions, the bath contained a low-calcium (0.18 mM) Ringer's. For selectivity experiments, a 0.1- $\mu\text{M}$  free calcium bath solution, buffered with EGTA, and a 1.8-mM calcium Ringers for the pipette, were made from a 100-mM calcium standard solution (Corning Medical and Scientific, Corning Glass Works, Medfield, MA). All patch experiments were performed at  $\sim 25^\circ\text{C}$ .

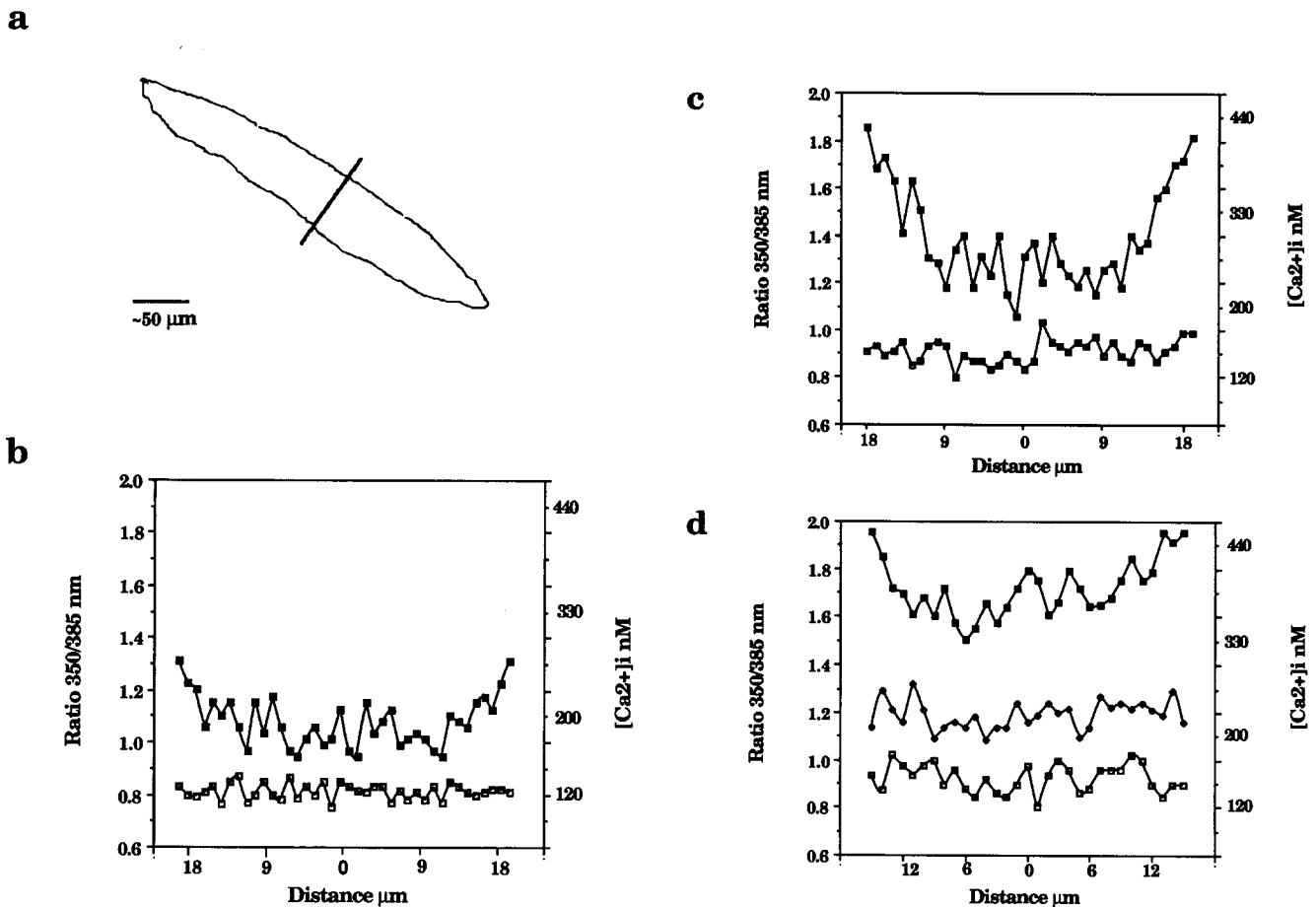


**Figure 1.** Free calcium levels were higher near the sarcolemma of stressed adult *mdx* fibers. (a) Schematic showing approximate location of optical sections across digitized ratio images of adult fibers. The *fdb* muscles were dissected intact from 3–6-wk-old normal and *mdx* mice, and loaded with the AM-ester form of fura-2. Bar,  $\sim 50 \mu\text{m}$ . (b) The fluorescence ratio (510 nm) from excitation at 350 and 385 nm, obtained every  $1 \mu\text{m}$  across a transverse section of a digitized image of a normal mouse *fdb* muscle fiber before ( $\square$ ) and 10 min after ( $\blacksquare$ )  $[\text{Ca}^{2+}]_o$  was elevated from 1.8 (normal) to 36 mM. Fibers were loaded with fura-2 AM for  $\sim 45$  min before recording.  $[\text{Ca}^{2+}]_i$  values shown were derived from the ratio values at each point.  $T = 37^\circ\text{C}$ . Fiber was  $40 \mu\text{m}$  in diameter. (c) Similar section across an *mdx* mouse *fdb* fiber before ( $\square$ ) and 10 min after ( $\blacksquare$ )  $[\text{Ca}^{2+}]_o$  was elevated from 1.8 to 36 mM.  $T = 37^\circ\text{C}$ . Fiber diameter was  $39 \mu\text{m}$ . The gradient at 10 min suggests that  $[\text{Ca}^{2+}]_i$  was greatly elevated near the sarcolemma of the fiber, and lower in the fiber interior. (d) Section across an *mdx* fiber before ( $\square$ ), 2 min ( $\blacksquare$ ), and 8 min ( $\blacklozenge$ ) after addition of a high  $\text{K}^+$  Ringer's (15 mM). At 2 min,  $[\text{Ca}^{2+}]_i$  was elevated throughout the fiber, but by 8 min  $[\text{Ca}^{2+}]_i$  had dropped.  $[\text{Ca}^{2+}]_o$  was 1.8 mM, and did not change for the duration of the experiment. Fiber diameter was  $32 \mu\text{m}$ .  $T = 37^\circ\text{C}$ .

## Results

### $[\text{Ca}^{2+}]_i$ Was Higher Near the Sarcolemma

Resting levels  $[\text{Ca}^{2+}]_i$  are elevated in *mdx* fibers (Turner et al., 1988; Williams et al., 1990) and in cultured DMD and *mdx* muscle (Mongini et al., 1988; Fong et al., 1990). Such elevations could be the result of increased calcium influx or reduced efflux across the sarcolemma and t-tubule system. Images of fura-2-loaded adult normal and *mdx* muscle fibers, in the presence of the normal  $[\text{Ca}^{2+}]_o$  of 1.8 mM, showed no regional differences in  $[\text{Ca}^{2+}]_i$  levels, although *mdx*  $[\text{Ca}^{2+}]_i$  levels were higher than normal (Fig. 1, b and c, open symbols). However, when  $[\text{Ca}^{2+}]_o$  was elevated to 36 mM,  $[\text{Ca}^{2+}]_i$  increased rapidly in *mdx* fibers (Fig. 1 c, closed symbols), but not to the same extent in normal fibers (Fig. 1 b). In both, the region of the largest initial calcium increase was near the sarcolemma. In *mdx* fibers, at  $t = 10$  min, with a  $[\text{Ca}^{2+}]_o$  of

36 mM, estimated  $[\text{Ca}^{2+}]_i$  in *mdx* fibers was  $385 \pm 42$  nM ( $n = 6$ ) near the sarcolemma, and  $240 \pm 27$  ( $n = 6$ ) in the fiber center (Fig. 1 c). Normal fiber  $[\text{Ca}^{2+}]_i$  was  $267 \pm 22$  ( $n = 8$ ) near the sarcolemma and  $184 \pm 16$  nM ( $n = 8$ ) near the center, at  $t = 10$  min (Fig. 1 b). By  $t = \sim 60$  min, the  $[\text{Ca}^{2+}]_i$  distribution was nearly uniform across both normal and *mdx* fibers: the average  $[\text{Ca}^{2+}]_i$  was  $209 \pm 29$  nM in eight normal and  $297 \pm 34$  nM in six *mdx* fibers.

Similar experiments in cultured myotubes did not show such specific regional changes in  $[\text{Ca}^{2+}]_i$ , only a more generalized  $[\text{Ca}^{2+}]_i$  increase which was more pronounced in dystrophic myotubes (data not shown, see Fong et al., 1990 for response of myotubes to  $[\text{Ca}^{2+}]_o$  of 18 mM).

When fibers were depolarized with 15 mM extracellular  $\text{K}^+$  ( $n = 2$  normal, 2 *mdx*),  $[\text{Ca}^{2+}]_i$  levels rose rapidly, but  $[\text{Ca}^{2+}]_i$  also increased throughout the fiber interior by  $t = 2$  min (Fig. 1 d). Therefore, the dye can respond to  $[\text{Ca}^{2+}]_i$  changes throughout the fiber interior.  $[\text{Ca}^{2+}]_i$  levels slowly

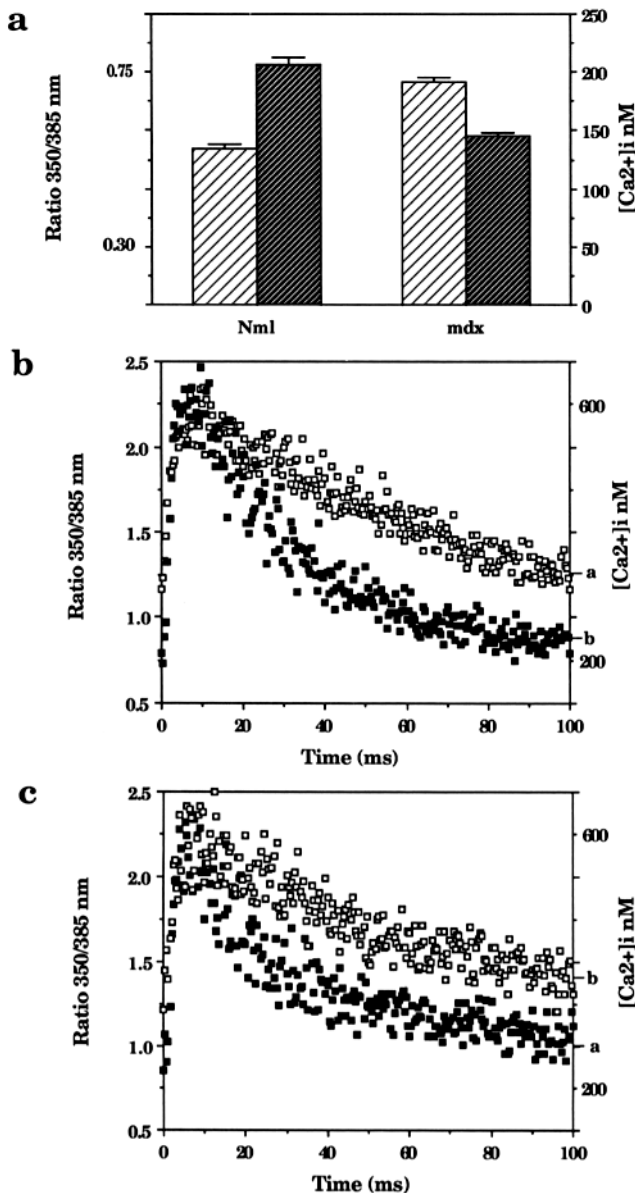


**Figure 2.** Resting  $[Ca^{2+}]_i$  determined calcium transient kinetics. (a) Adult mouse *fib* fibers were loaded with fura-2 AM for  $\sim 45$  min. For normal fibers,  $[Ca^{2+}]_o$  was elevated from 1.8 to 36 mM, and for *mdx* fibers,  $[Ca^{2+}]_o$  was lowered from 1.8 to 0.18 mM. Mean resting unstimulated  $[Ca^{2+}]_i$  levels are shown before (light bars) and after (dark bars) they had reached stable new levels.  $n = 20$  normal (*Nml*) and 22 *mdx* fibers ( $\pm$ SEM).  $T = 25^\circ C$ . (b) Ratio averaged calcium transients from a normal fiber before ( $\blacksquare$ ) and after ( $\square$ )  $[Ca^{2+}]_i$  was elevated to *mdx* levels. Fiber was stimulated at 3.3 Hz, and 100 transients were averaged for each data point, at an initial resolution of 100  $\mu s$  per point. One point every 0.4 ms is displayed.  $T = 25^\circ C$ . The basal steady state calcium levels at 100 ms during stimulation before (b) and after (a)  $[Ca^{2+}]_i$  elevation are indicated on the ratio scale for comparison with the unstimulated resting levels shown in Fig. 2a. (c) Calcium transients from an *mdx* fiber before ( $\square$ ) and after ( $\blacksquare$ )  $[Ca^{2+}]_i$  was lowered to near normal levels. 50 transients were averaged for each point, and the traces therefore were noisier than in Fig. 2b. Fiber was stimulated at 3.3 Hz,  $T = 25^\circ C$ . Basal calcium levels at 100 ms during stimulation are again indicated on the ratio scale, both before (b) and after (a)  $[Ca^{2+}]_i$  was lowered.

returned toward normal levels (Fig. 1 d), presumably as voltage-gated calcium channels inactivated.

### Transient Kinetics Depends on $[Ca^{2+}]_i$

Calcium transients are prolonged in *mdx* fibers (Turner et al., 1988). This result suggested that calcium sequestration mechanisms, or a combination of release and sequestration, may be altered in dystrophic fibers. Sequestration could be slowed as a result of reduced sarcoplasmic reticulum  $Ca^{2+}$ -ATPase activity, reduced buffering of cytosolic calcium by a lowered parvalbumin content, or reduced calcium efflux across the cell surface. Alternatively, calcium sequestration mechanisms may be undamaged in *mdx* fibers, but their activity could be slowed as a result of the elevated  $[Ca^{2+}]_i$ . Since it is possible to alter  $[Ca^{2+}]_i$  levels in fibers by changing  $[Ca^{2+}]_o$  (Turner et al., 1988), we were able to test this hypothesis by measuring transients before and after resting  $[Ca^{2+}]_i$  levels were reset in normal and *mdx* fibers.

Freshly dissected *fib* muscle fibers were loaded with fura-2 AM for 30–45 min in normal Ringer's (1.8 mM  $[Ca^{2+}]_o$ ) and resting  $[Ca^{2+}]_i$  was monitored. After dye loading, normal fibers were incubated in a 36-mM  $[Ca^{2+}]_o$  Ringer's. Resting  $[Ca^{2+}]_i$  levels rose slowly over a period of 20–30 minutes, and finally reached those of *mdx* fibers (Fig. 1 b and Fig. 2 a). Fibers were then placed in normal Ringer's. Before and after  $[Ca^{2+}]_i$  elevation, fibers were stimulated electrically, and calcium transients were recorded (Materials and Methods, Turner et al., 1988).

Transients were initially rapid, but were slower after  $[Ca^{2+}]_i$  had been elevated (Fig. 2 b). Transient decay half-times ( $t_{1/2}$ ) increased significantly from  $\sim 10$  to 17 ms at  $37^\circ C$  (Table I). During repetitive stimulation,  $[Ca^{2+}]_i$  levels do not return to the prestimulus resting levels, but remain elevated (Klein et al., 1988; Turner et al., 1988). This elevation can be seen by comparing the basal or steady-state level measured at 100 ms during stimulation (*-a* and *-b* in Fig. 2 b) with the unstimulated resting levels (Fig. 2 a). The basal elevation was higher in normal fibers after the resting  $[Ca^{2+}]_i$  elevation. Transient kinetics became more rapid as resting  $[Ca^{2+}]_i$  levels slowly returned to normal after the reintroduction of normal Ringer's (data not shown).

Conversely, transients in *mdx* muscle were measured before and after incubation in a reduced (0.18 mM) calcium Ringer's. Under these conditions  $[Ca^{2+}]_i$  levels slowly approached those of normal fibers (Fig. 2 a). Transient decay rates became more rapid as  $[Ca^{2+}]_i$  fell (Fig. 2 c and Table I).  $t_{1/2}$  dropped significantly from 17 to 11 ms at  $37^\circ C$ . Basal  $[Ca^{2+}]_i$  levels during stimulation were also lower after incubation in reduced calcium Ringer's (compare *-a* and *-b*, Fig. 2 c). As in normal fibers, the effect on *mdx* transient duration was reversible. Thus, transient kinetics varied directly with resting  $[Ca^{2+}]_i$ , and transient decay rates in normal and dystrophic fibers were identical when  $[Ca^{2+}]_i$  levels were similar.

### Transient Peak Heights Were Identical in Normal and *mdx* Fibers

Fibers were stimulated at  $\leq 3.3$  Hz, since these frequencies produced maximal transient peak heights. Peak  $[Ca^{2+}]_i$  levels appeared identical in normal and *mdx* fibers when measured with fura-2:  $\sim 0.6 \mu M$  at  $25^\circ C$ ,  $1.1 \mu M$  at  $37^\circ C$  (Table

Table I. Fura-2 Calcium Transient Data ( $\pm$  SEM)

Fiber	$^{\circ}\text{C}$	Peak ( $\mu\text{M}$ )	Peak time	Decay $t_{1/2}$	$n$	Ratios†
		$\mu\text{M}$	$\text{ms}$	$\text{ms}$		
Normal	37	1.148 $\pm$ 0.123	3.75 $\pm$ 0.26	9.70 $\pm$ 0.70	10	580
	25	0.617 $\pm$ 0.029	5.31 $\pm$ 0.14	27.28 $\pm$ 1.38	24	710
Normal (Hi)‡	37	1.045 $\pm$ 0.080	4.59 $\pm$ 0.58	17.10 $\pm$ 0.70	4	450
	25	0.664 $\pm$ 0.087	6.01 $\pm$ 0.38	40.70 $\pm$ 2.95	7	400
<i>mdx</i>	37	1.217 $\pm$ 0.026	4.27 $\pm$ 0.58	15.53 $\pm$ 1.39	7	510
	25	0.589 $\pm$ 0.120	6.88 $\pm$ 0.25	38.71 $\pm$ 1.73	33	1980
<i>mdx</i> (Lo)‡	37	1.188 $\pm$ 0.089	3.65 $\pm$ 0.34	11.20 $\pm$ 1.20	4	450
	25	0.658 $\pm$ 0.078	6.06 $\pm$ 0.39	24.75 $\pm$ 3.33	10	1350

\* Transient decay  $t_{1/2}$  was determined graphically as the duration in which the response dropped 50% from the peak towards the level at the end of the 100-ms sampling period.

‡ Number of transients that were ratio averaged to obtain values.

§ Normal fibers, after  $[\text{Ca}^{2+}]_i$  was elevated to *mdx* levels.

|| *mdx* fibers, after  $[\text{Ca}^{2+}]_i$  was lowered to near normal levels.

I; Turner et al., 1988). However, since fura-2 signals begin to saturate at micromolar free calcium levels (Grynkiwicz et al., 1985), transient peak  $[\text{Ca}^{2+}]_i$  levels were checked using another calcium-sensitive dye, fluo-3 (Minta et al., 1989). The weaker binding of calcium by fluo-3 ( $k_d \sim 450$  nM at  $37^{\circ}\text{C}$  compared with  $\sim 175$  nM for fura-2) facilitates measurements of higher peak calcium values than is possible with fura-2. Fluo-3 exhibits a 40-fold increase in fluorescence emission at 526 nm after chelating calcium, and the signal cannot be ratio averaged, so extra care had to be taken to prevent movement artifacts (see Materials and Methods).

We found that fluo-3 transients were similar to those obtained with fura-2. The transient  $t_{1/2}$  values in *mdx* fibers were again significantly longer than  $t_{1/2}$  in normal fibers. Mean values ( $\pm$ SEM) were  $19.4 \pm 0.3$  ms for two *mdx* vs.  $11.6 \pm 0.23$  for three normal fibers at  $37^{\circ}\text{C}$ , and  $52.0 \pm 4$  ms for two *mdx* vs.  $35.7 \pm 0.7$  ms for three normal fibers at  $25^{\circ}\text{C}$ . The calculated peak calcium values were not significantly different from those found using fura-2, being  $0.600 \pm 0.08 \mu\text{M}$  in *mdx* with fluo-3 ( $n = 3$ ) compared with  $0.589 \pm 0.120 \mu\text{M}$  ( $n = 33$ ) with fura-2 in *mdx* mice, at  $25^{\circ}\text{C}$  (Table I). Times to peak were also similar to those obtained with fura-2. Mean values ( $\pm$ SEM) were  $3.20 \pm 0.60$  ms in three normal and two *mdx* fibers at  $37^{\circ}\text{C}$ , and  $6.24 \pm 0.36$  in three normal and two *mdx* fibers at  $25^{\circ}\text{C}$ .

In contrast to reports where the majority of AM-ester-loaded dye is found to be responsive in muscle (Iaizzo et al., 1989), we estimate that as much as 50% or more of AM-ester-loaded fura-2 may be unresponsive in adult fibers (Baylor and Hollingsworth, 1988; Turner et al., 1988). Similar amounts of unresponsive fluo-3 AM-ester were also present. However, the effects on the signal from unresponsive dye were included in the calibrations, and the similarities between normal and *mdx* peak calcium values obtained using the lower affinity fluo-3 and the higher affinity fura-2 lead us to conclude that peak heights were similar in normal and *mdx* fibers.

### Free Sodium Levels Were Not Different

The elevated  $[\text{Ca}^{2+}]_i$  observed in dystrophic cells could be the result of a nonspecific cation leak in the sarcolemma. Such a leak would result in an increased permeability to sodium ions, and perhaps an increase in resting ( $[\text{Na}^+]_i$ ) lev-

els. To measure resting  $[\text{Na}^+]_i$  levels and the permeability of the sarcolemma to sodium, the sodium dye SBFI was AM-ester loaded or injected into fibers and myotubes. SBFI has similar excitation and emission properties to fura-2 (Harootunian et al., 1989).

The dye response to varied  $[\text{Na}^+]_o$ , in the presence of ionophores, was used to calibrate the dye in vivo (Fig. 3 a). The calibration curves for SBFI in AM-ester-loaded fibers and myotubes, and fibers microinjected with SBFI-free acid, were similar in form (Fig. 3 b). Microinjected dye was found to be more responsive than ester-loaded dye. Only  $\sim 30\%$  of the microinjected dye, but perhaps 50% of AM-ester-loaded SBFI, was not responsive during the in vivo calibrations (data not shown). Uncleaved AM-ester and bound dye may therefore be present and dye may enter other intracellular compartments (Harootunian et al., 1989). Over 90% of the dye was rapidly lost after treatment with  $140 \mu\text{M}$  digitonin, and similar concentrations of digitonin have been shown to release dye from the cytosol and other intracellular compartments (Roe et al., 1990).

Resting ratios from ester-loaded normal and dystrophic cells were identical, with the approximate  $[\text{Na}^+]_i$  being  $\sim 10$  mM for all cell types at  $37^{\circ}\text{C}$  (Table II). Dye concentrations in cells varied between 10 and  $50 \mu\text{M}$ , and ratios obtained did not vary within this concentration range. Cells at  $25^{\circ}\text{C}$  had higher resting  $[\text{Na}^+]_i$  levels than at  $37^{\circ}\text{C}$  (Table II). After injection of SBFI into single skeletal muscle fibers, the ratio was initially elevated, but dropped to a stable baseline as the fiber recovered (Fig. 4 a). Dye concentration in injected fibers was  $\sim 50 \mu\text{M}$ . Resting ratios in *mdx* and normal fibers were again identical and corresponded to resting  $[\text{Na}^+]_i$  values of  $\sim 10$  mM (Table II).

Fiber  $[\text{Na}^+]_i$  was also estimated using sodium-selective microelectrodes. Only experiments with electrodes whose response to a 10-fold variation in free sodium was  $\sim 59 \pm 5$  mV at  $25^{\circ}\text{C}$ , both before and after an experiment, were acceptable. The fiber resting potential was measured with a second conventional microelectrode filled with 3 M KCl: this potential was subtracted from the sodium electrode signal. Using this method, fiber  $[\text{Na}^+]_i$  was estimated to be  $10 \pm 5$  mM in three normal fibers.

### Sodium Influx Rates Were Identical

An increased rate of sodium entry into dystrophic fibers and

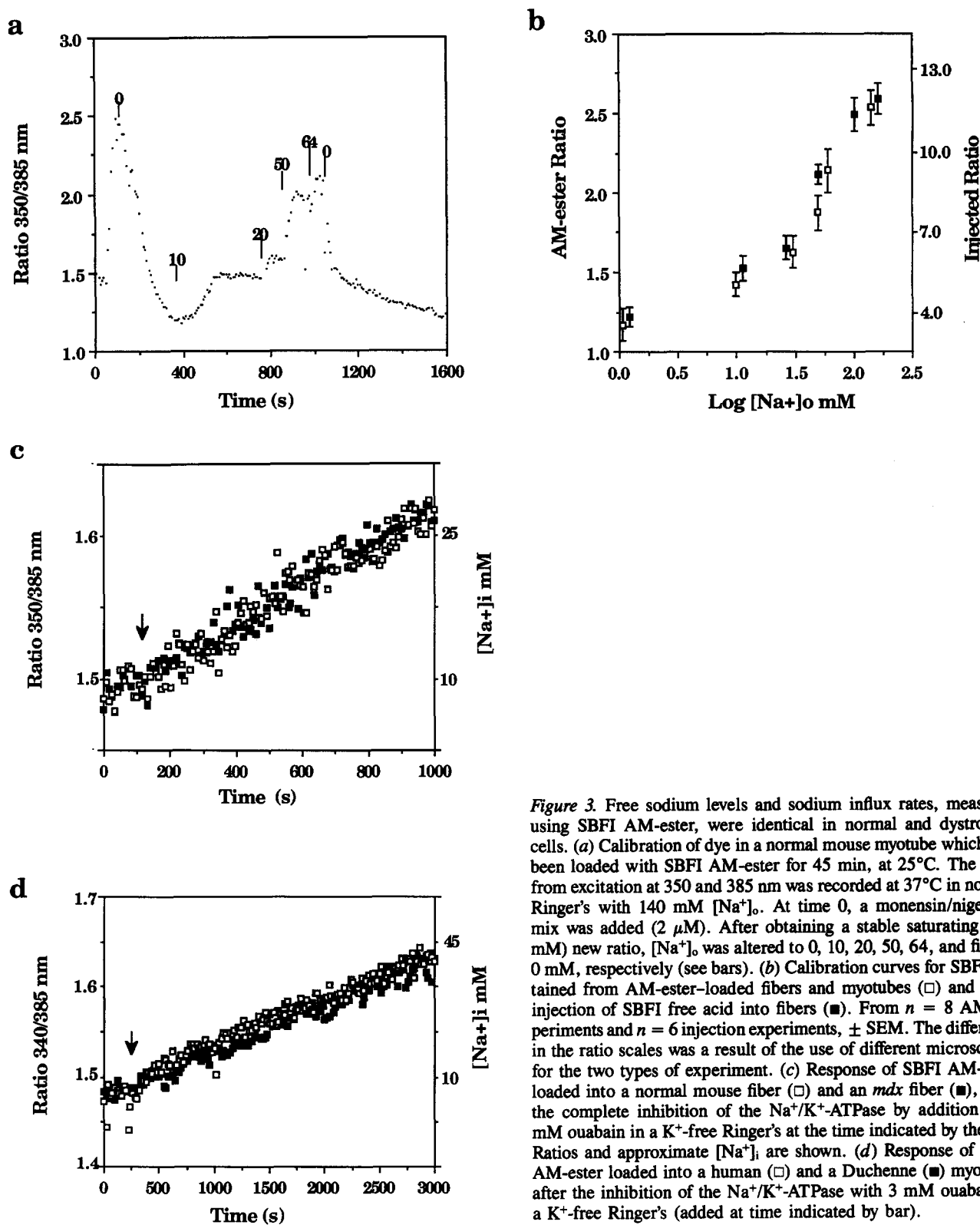


**Figure 3.** Free sodium levels and sodium influx rates, measured using SBF AM-ester, were identical in normal and dystrophic cells. (a) Calibration of dye in a normal mouse myotube which had been loaded with SBF AM-ester for 45 min, at 25°C. The ratio from excitation at 350 and 385 nm was recorded at 37°C in normal Ringer's with 140 mM  $[Na^+]_o$ . At time 0, a monensin/nigericin mix was added (2  $\mu$ M). After obtaining a stable saturating (140 mM) new ratio,  $[Na^+]_o$  was altered to 0, 10, 20, 50, 64, and finally 0 mM, respectively (see bars). (b) Calibration curves for SBF obtained from AM-ester-loaded fibers and myotubes ( $\square$ ) and from injection of SBF free acid into fibers ( $\blacksquare$ ). From  $n = 8$  AM experiments and  $n = 6$  injection experiments,  $\pm$  SEM. The difference in the ratio scales was a result of the use of different microscopes for the two types of experiment. (c) Response of SBF AM-ester loaded into a normal mouse fiber ( $\square$ ) and an *mdx* fiber ( $\blacksquare$ ), after the complete inhibition of the  $Na^+/K^+$ -ATPase by addition of 3 mM ouabain in a  $K^+$ -free Ringer's at the time indicated by the bar. Ratios and approximate  $[Na^+]_i$  are shown. (d) Response of SBF AM-ester loaded into a human ( $\square$ ) and a Duchenne ( $\blacksquare$ ) myotube, after the inhibition of the  $Na^+/K^+$ -ATPase with 3 mM ouabain in a  $K^+$ -free Ringer's (added at time indicated by bar).

myotubes might not result in a change in resting  $[Na^+]_i$ , because of a possible compensatory increase in the activity of the  $Na^+/K^+$ -ATPase. Therefore, the initial rate of  $[Na^+]_i$  increase, after the complete inhibition of the  $Na^+/K^+$  ATPase with 3 mM ouabain in a  $K^+$ -free Ringer's, was also measured.

The initial rate of  $[Na^+]_i$  increase in both *mdx* and normal adult fibers was identical:  $\sim 1$  mM/min at 37°C (Table II), and did not depend on the method of dye loading. Normal and dystrophic  $[Na^+]_i$  influx rates in cultured mouse and human myotubes were also identical, but rates were  $\sim 30\%$  lower than in adult fibers (Table II). Influx rates were maxi-

Table II. Resting  $[Na^+]_i$  and  $Na^+$  Influx Rates

Cell type	°C	Loading*	$[Na^+]_i$ ‡	n	Flux‡	n
<i>mdx</i> fibers	37	Injected	$10.0 \pm 2.7$	6	$1.08 \pm 0.20$	2
	37	AM	$10.3 \pm 1.2$	15	$1.05 \pm 0.05$	8
	25	Injected	$9.8 \pm 2.5$	7	-	-
	25	AM	$13.8 \pm 1.5$	21	$0.91 \pm 0.15$	5
Normal fibers	37	Injected	$10.8 \pm 2.7$	6	$1.15 \pm 0.15$	2
	37	AM	$10.6 \pm 1.7$	16	$1.05 \pm 0.06$	8
	25	Injected	$10.1 \pm 1.7$	15	-	-
	25	AM	$12.7 \pm 1.6$	20	$0.95 \pm 0.12$	6
<i>mdx</i> myotubes	37	AM	$9.2 \pm 1.8$	18	$0.89 \pm 0.09$	6
	25	AM	$11.3 \pm 2.8$	10	$0.65 \pm 0.07$	7
Normal myotubes	37	AM	$9.6 \pm 1.7$	11	$0.93 \pm 0.11$	5
	25	AM	$12.3 \pm 1.9$	10	$0.69 \pm 0.10$	6
DMD myotubes	37	AM	$9.7 \pm 1.8$	16	$0.71 \pm 0.08$	7
Human myotubes	37	AM	$10.5 \pm 1.6$	17	$0.69 \pm 0.10$	6

\* The adult fibers were microinjected with  $\sim 50 \mu M$  dye, and loaded using the AM-ester. The myotubes were AM-ester loaded only.

‡ Resting  $[Na^+]_i$  values (in mM)  $\pm$  SEM were estimated from the calibration curves. Separate curves were obtained for each cell type: adult fibers with injected dye, adult fibers AM-ester loaded, and myotubes AM-ester loaded.

§ The initial (maximal) rate of  $[Na^+]_i$  increase, in mM/min ( $\pm$  SEM) immediately after the complete inhibition of the  $Na^+/K^+$ -ATPase with a  $0 K^+$  Ringer containing 3 mM ouabain.

mal shortly after the addition of the ouabain/ $0 mM K^+$  Ringer's, but gradually slowed as the sodium concentration gradient dissipated (Fig. 3, *c* and *d*, and Fig. 4 *a*). The  $[Na^+]_i$  levels slowly returned to normal after the ouabain was removed with several washes with normal Ringer's (Fig. 4 *a*). The lower sodium influx rates obtained in cultured myotubes compared with rates in adult fibers (Table II) may be a result of cell adhesion to the bottom of the dish, which might reduce the cell surface area available for sodium ion influx.

### Leak Channels Are Selective for Calcium

We have described previously the presence of spontaneously active channels, in normal and dystrophic myotubes, that conduct barium and calcium (Fong et al., 1990). We recorded the activity of this channel in cultured human and mouse myotubes for longer periods of time (up to  $\sim 2$  min vs.  $\sim 4$  s previously), and activity was again significantly higher in *mdx* and Duchenne myotubes than normal (Fig. 5 *a*). The  $P_o$  did not depend on membrane potential (Fig. 5

*b*). The differences in  $P_o$  were also observed after cell-attached patches were excised to form "inside-out" patches. Mean  $P_o$  values ( $\pm$  SEM) were  $0.035 \pm 0.004$  in 106 normal mouse records,  $0.078 \pm 0.008$  in 81 *mdx* records,  $0.046 \pm 0.010$  in 13 human, and  $0.101 \pm 0.011$  in 49 DMD records. The higher  $P_o$  in dystrophic myotubes is the result of reduced mean channel closed times, mean open times being the same in both normal and dystrophic myotubes (data not shown; for leak channel kinetics see Fong et al., 1990).

We have examined leak channel activity with a high barium or calcium solution in the pipette (108 mM total divalent ion, sodium free). Single channel currents measured in the presence of either barium or calcium had similar amplitudes and conductance ( $\sim 10$  pS; Fong et al., 1990). However, under physiological conditions, sodium could be the major cation entering myotubes via these channels. To test channel selectivity directly, we measured single channel leak currents in excised "inside-out" patches with standard Ringer's in the pipette (1.8 mM  $Ca^{2+}$ ), and 0.1  $\mu M$  free calcium in the bath. This calcium concentration was chosen to approximate the cytosolic  $[Ca^{2+}]_i$  in fibers and myotubes at rest.

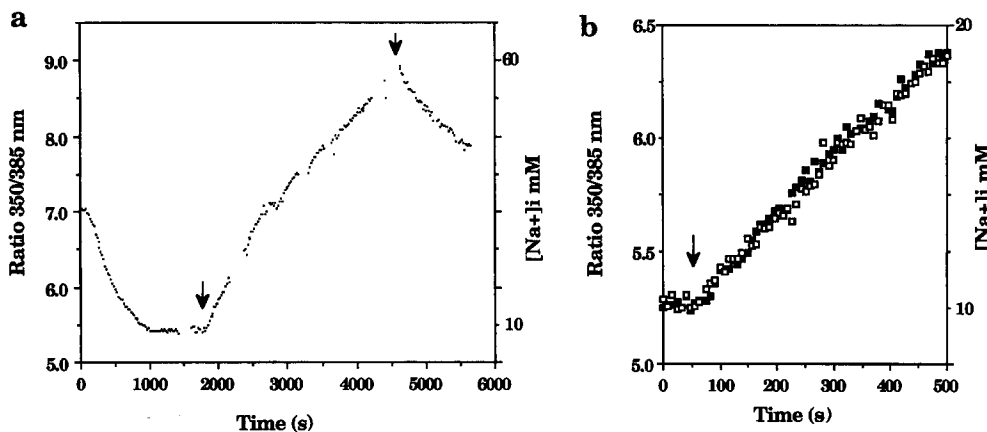
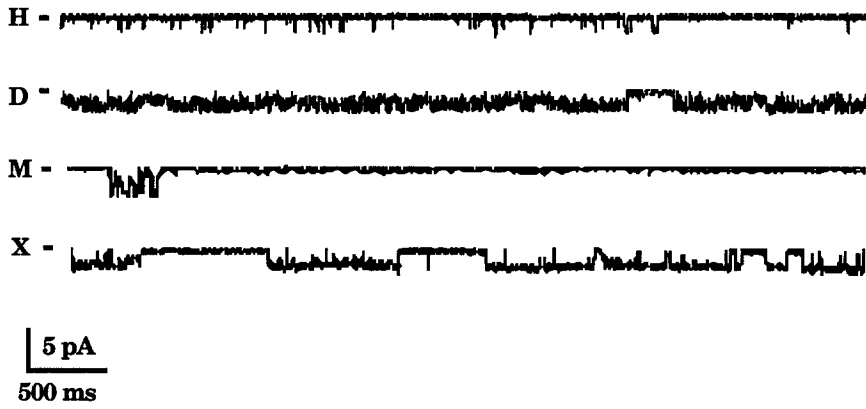
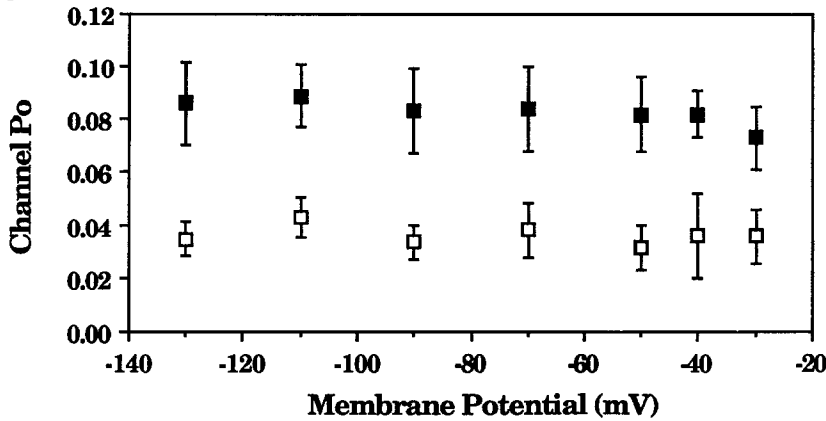
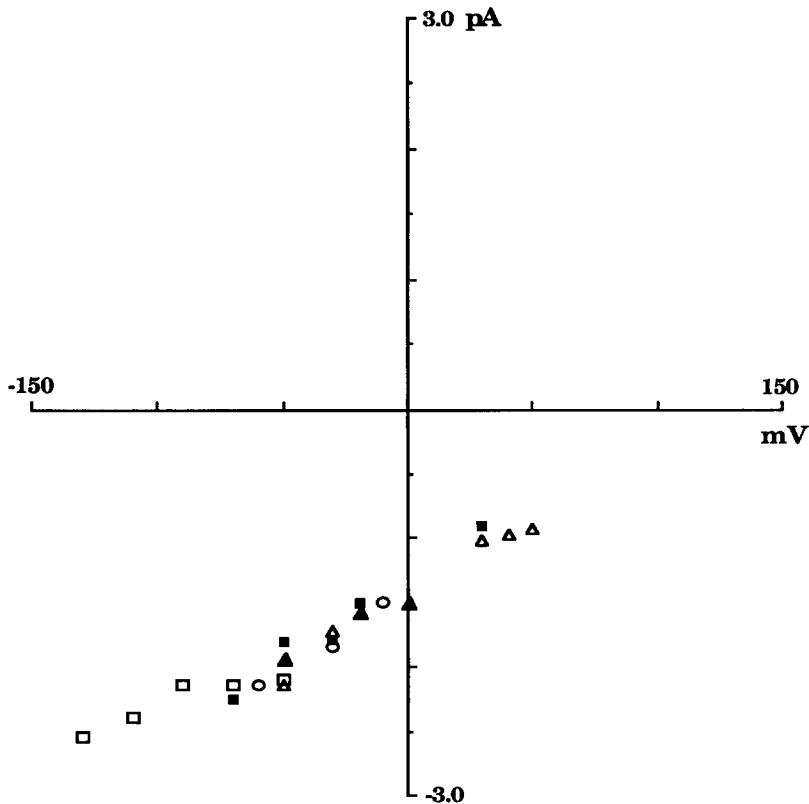
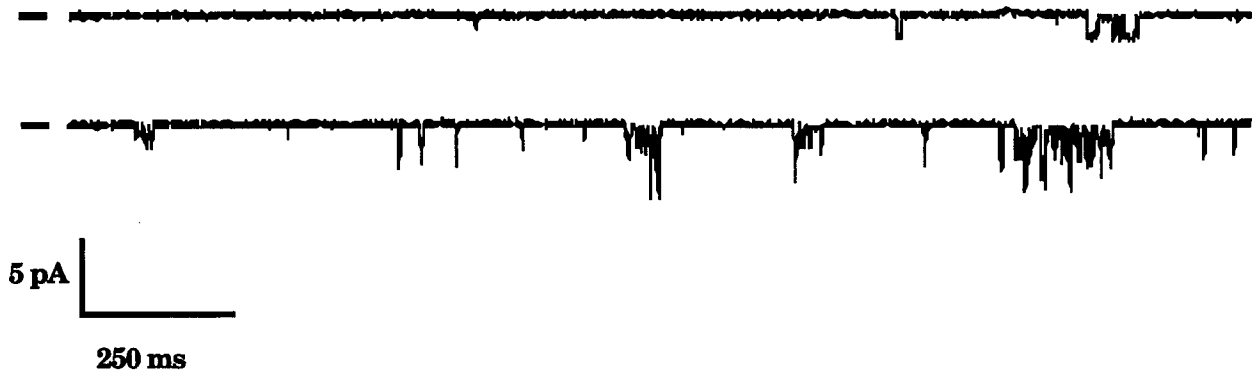
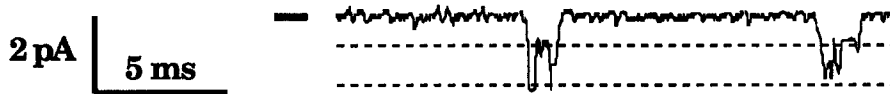
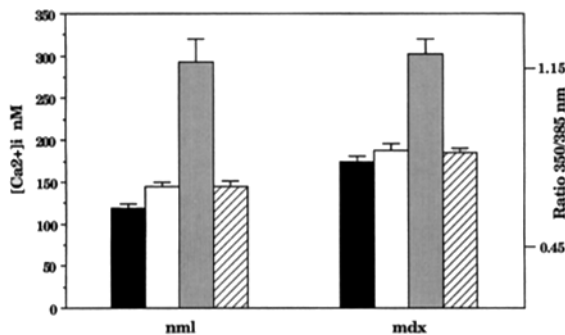


Figure 4. Free sodium levels and sodium influx rates, measured with microinjected SBFI, were identical in normal and *mdx* fibers. (a) Ratio and approximate  $[Na^+]_i$  in a single fiber from a normal mouse *fdb* muscle injected at time 0 with  $<1\%$  cell volume of a solution containing SBFI free acid. After the fiber recovered and a stable baseline was obtained, the fiber was exposed to a Ringer's containing  $0 mM K^+$  and  $3 mM$  ouabain, to inhibit the  $Na^+/K^+$ -ATPase (first arrow). Ouabain was washed out

with normal Ringer's (second arrow). (b) Comparison of the initial sodium influx rates after the complete inhibition of the  $Na^+/K^+$ -ATPase in a normal ( $\square$ ) and an *mdx* ( $\blacksquare$ ) fiber, both injected with SBFI free acid. Ouabain Ringer's was added at time indicated by the bar.

**a****b****c**

**Figure 5.** Leak channels were more active in dystrophic myotubes, and were selective for calcium. (a) Leak channel activity in cell-attached patches obtained from normal and dystrophic myotubes. Channels were more active in dystrophic than normal myotubes, in both cell-attached patches and after excision to form inside-out patches (data not shown). Data was acquired at 1.5 kHz and filtered at 1 kHz during playback. Pipette contained 96 mM  $Ba^{2+}$  (Materials and Methods). Bars to the left of records indicate closed state levels. Inward current is down in these records. Records are from normal human (H), Duchenne human (D), normal mouse (M), and dystrophic mouse (X) myotubes. Holding potential for all records was  $-110$  mV. (b) Leak channel  $P_o$  plotted against the membrane holding potential in patches from normal ( $\square$ ) and *mdx* ( $\blacksquare$ ) mouse myotubes. Mean channel open and closed time histograms were generated by pClamp analysis of data files, and  $P_o$  values ( $\pm$ SEM) were derived from the relationship  $P_o = \text{mean open time} / (\text{mean open time} + \text{mean closed time})$ . Data was from a total of 106 normal and 81 *mdx* records.  $P_o$  in DMD and normal human myotubes was also potential independent (data not shown). (c) Current-voltage relationship showing mean currents obtained from three excised normal mouse myotube patches (open symbols) and two excised *mdx* mouse myotube patches (solid symbols). Pipette contained 150 mM  $Na^+$ , 1.8 mM  $Ca^{2+}$ , 155 mM  $Cl^-$ , 2.7 mM  $K^+$ , and 1.0 mM  $Mg^{2+}$ . Bath contained 152 mM  $Na^+$ , and 0.1  $\mu$ M  $Ca^{2+}$ , 155 mM  $Cl^-$ , 2.7 mM  $K^+$ , and 1.0 mM  $Mg^{2+}$ . Predicted  $E_{rev}$  for  $Na^+$ ,  $K^+$ , and  $Cl^-$  was  $\sim 0$  mV, and the predicted  $E_{rev}$  for  $Ca^{2+}$  was  $+127$  mV under these conditions.

**a****b****c**

compared with the expected  $\sim 0.03\%$ , and to a third level was  $1.5\%$  compared with  $0.0004\%$  expected for independent channel openings. (c) The effects of nifedipine and Bay K 8644 on resting  $[Ca^{2+}]_i$  in normal and *mdx* myotubes. Cells were loaded with fura-2 AM, and resting  $[Ca^{2+}]_i$  measured in normal Ringer's (solid bars,  $n = 10$  normal (*nml*) and  $10$  *mdx*),  $T = 37^\circ\text{C}$ . Cells were then exposed to Ringer's containing  $10 \mu\text{M}$  nifedipine (open bars,  $n = 4$  normal,  $3$  *mdx*),  $50 \mu\text{M}$  nifedipine (shaded bars,  $n = 6$  normal,  $8$  *mdx*), or  $50 \mu\text{M}$  Bay K 8644 (striped bars,  $n = 4$  normal and  $4$  *mdx*). Fura-2 signals were monitored until changes in  $[Ca^{2+}]_i$  had stabilized, or for up to  $\sim 30$  min.

The extrapolated reversal potentials ( $E_{\text{rev}}$ ) obtained under these conditions were always at least  $+100$  mV, and closer to the  $+127$  mV  $E_{\text{rev}}$  predicted for a calcium-selective channel (Fig. 5 c), than the  $E_{\text{rev}}$  for  $\text{Na}^+$ ,  $\text{K}^+$ , and  $\text{Cl}^-$  ( $0$  mV under these conditions). With  $0.18$  mM calcium in the bath, and a  $\text{Ca}^{2+}$   $E_{\text{rev}}$  of  $+29$  mV, the estimated reversal potential remained positive ( $11$  normal,  $7$  *mdx* records, data not shown).

If the channel conducts sodium under physiological conditions, we would expect to see a change in  $E_{\text{rev}}$  and current amplitudes when pipette free sodium concentration is altered and pipette free calcium concentration is held constant ( $1.8$  mM). However, when pipette free sodium concentration was lowered to  $70$  mM from  $150$  mM, the unitary amplitudes did not change: mean inward currents with either  $70$  or  $150$  mM pipette free sodium concentration were  $1.1$  pA at  $-50$  mV,  $1.2$  pA at  $-70$  mV, and  $1.4$  pA at  $-90$  mV (eight normal, seven *mdx* mouse records), and the  $E_{\text{rev}}$  was unaltered (data not shown).

**Figure 6.** Increased leak channel activity resulted in elevated  $[Ca^{2+}]_i$ . (a) Channel activity was increased by nifedipine in cell-attached patches from normal and *mdx* mouse myotubes. Pipette contained  $96$  mM  $\text{Ba}^{2+}$  in upper (control) record and  $96$  mM  $\text{Ba}^{2+}$  plus  $50 \mu\text{M}$  nifedipine in lower trace. Both records shown are from a normal mouse myotube. Holding potential was  $\sim -110$  mV. Data was acquired at  $1.5$  kHz and filtered at  $1$  kHz on playback. (b) Expanded portion of nifedipine trace shown above. Nifedipine appeared to act by increasing both the  $P_o$  and the conductance of the channel to two and three (or more) times the unitary conductance. In this record, the observed probability of opening to a higher conductance level was much greater than would be expected by binomial theory for four channels opening independently in the patch: the observed rate of transition to a second level was  $1.9\%$

compared with the expected  $\sim 0.03\%$ , and to a third level was  $1.5\%$  compared with  $0.0004\%$  expected for independent channel openings. (c) The effects of nifedipine and Bay K 8644 on resting  $[Ca^{2+}]_i$  in normal and *mdx* myotubes. Cells were loaded with fura-2 AM, and resting  $[Ca^{2+}]_i$  measured in normal Ringer's (solid bars,  $n = 10$  normal (*nml*) and  $10$  *mdx*),  $T = 37^\circ\text{C}$ . Cells were then exposed to Ringer's containing  $10 \mu\text{M}$  nifedipine (open bars,  $n = 4$  normal,  $3$  *mdx*),  $50 \mu\text{M}$  nifedipine (shaded bars,  $n = 6$  normal,  $8$  *mdx*), or  $50 \mu\text{M}$  Bay K 8644 (striped bars,  $n = 4$  normal and  $4$  *mdx*). Fura-2 signals were monitored until changes in  $[Ca^{2+}]_i$  had stabilized, or for up to  $\sim 30$  min.

With only sodium chloride in the pipette, small inward single-channel currents were observed: from  $0.61$  pA at  $-80$  mV to  $0.86$  pA at  $-120$  mV (five DMD and five normal human records). The channel conductance was therefore lower under these conditions ( $\sim 6$  pS). The  $P_o$  was not significantly different with only sodium present in the pipette ( $0.129 \pm 0.045$  in 5 DMD records with  $\text{Na}^+$  compared with  $0.101 \pm 0.011$  in 49 DMD records with  $\text{Ca}^{2+}$  and  $\text{Ba}^{2+}$ ). Channel kinetics also appeared unaltered (data not shown). These results suggest that the channel was permeable to sodium only in the absence of calcium, a property shared by other calcium channels (Edwards, 1982).

#### **Increasing Leak Channel Activity Elevates $[Ca^{2+}]_i$**

High concentrations of nifedipine acted as an agonist on leak channel activity. For each experiment, the untreated  $P_o$  was obtained before the addition of the drug. Lower ( $10 \mu\text{M}$ ) con-

centrations of nifedipine had little effect on channel  $P_o$  (data not shown). However, with 50  $\mu\text{M}$  nifedipine in the patch pipette, the  $P_o$  of leak channels in normal and dystrophic patches was increased (Fig. 6 a), and the channel entered multiconductance states (Fig. 6 b). The observed frequency of multiconductance levels was significantly greater than the frequency predicted by binomial theory for several channels opening independently in the same patch. With 50  $\mu\text{M}$  nifedipine,  $P_o$  increased significantly from  $0.024 \pm 0.007$  to  $0.059 \pm 0.010$  in 29 normal records and from  $0.077 \pm 0.021$  to  $0.197 \pm 0.054$  in 8 *mdx* records. These increases in  $P_o$  are averages and may be underestimates. In some records immediately after drug addition the  $P_o$  was unaltered, whereas in some later records the  $P_o$  was as much as 20–30 times higher.

In separate experiments, 10  $\mu\text{M}$  nifedipine only increased  $[\text{Ca}^{2+}]_i$  levels in normal and *mdx* myotubes by small amounts (Fig. 6 c), and had a similar small effect on adult muscle fibers (from  $124 \pm 3$  nM to  $137 \pm 2$  nM in three normal fibers). However, 50  $\mu\text{M}$  nifedipine resulted in larger increases in  $[\text{Ca}^{2+}]_i$  in myotubes (Fig. 6 c), and adult fibers (levels rose to  $374 \pm 25$  nM in three normal fibers). Both  $P_o$  and  $[\text{Ca}^{2+}]_i$  increases occurred slowly, over a period of minutes.

Stretch has been shown to alter the activity of channels in patches from normal and *mdx* myotubes (Franco and Lansman, 1990a). Therefore,  $[\text{Ca}^{2+}]_i$  in normal and *mdx* adult fibers, loaded with fura-2 AM, was monitored before and after fibers were stretched from a resting length of  $\sim 2.0$  to  $\sim 3.0$   $\mu\text{M}$  per sarcomere. Different results were obtained from the two fiber types. In normal fibers, at 25°C, resting  $[\text{Ca}^{2+}]_i$  was  $133 \pm 4.1$  nM. When the fiber was stretched,  $[\text{Ca}^{2+}]_i$  rose slightly to  $147 \pm 2.7$  nM ( $n = 13$ ), possibly as a result of stretch-gated leak channel openings. In *mdx* fibers,  $[\text{Ca}^{2+}]_i$  fell from  $175 \pm 5.2$  nM to  $167 \pm 1.6$  nM ( $n = 14$ ), possibly as a result of stretch-gated leak channel closures.

The dihydropyridine analogue Bay K 8644, an agonist of the cardiac myocyte calcium leak channel (Coulombe et al., 1989), did not increase leak channel  $P_o$ . With a concentration of 10  $\mu\text{M}$  in the pipette,  $P_o$  was  $0.039 \pm 0.009$  in five normal and  $0.061 \pm 0.021$  in three *mdx* records. Little effect on  $[\text{Ca}^{2+}]_i$  was seen in normal and *mdx* myotubes with 10 or 50  $\mu\text{M}$  (Fig. 6c) Bay K 8644.

Increased calcium influx into dystrophic muscle might occur via voltage-gated channels. The L-type calcium channel blockers verapamil (5  $\mu\text{M}$ ) and diltiazam (5  $\mu\text{M}$ ), as well as nifedipine (5  $\mu\text{M}$ ), did not lower resting  $[\text{Ca}^{2+}]_i$  levels in *mdx* fibers ( $n = 4$  fibers with each drug) or dystrophic myotubes ( $n = 6$ ). The voltage-gated channel agonist, Bay K 8644 (10–50  $\mu\text{M}$ ) also had little effect on resting  $[\text{Ca}^{2+}]_i$  levels (see above).

## Discussion

The absence of dystrophin in DMD humans and *mdx* mice results in the more frequent opening of calcium leak channels in the sarcolemma. It is our hypothesis that increased calcium influx via these channels results in the elevated  $[\text{Ca}^{2+}]_i$  seen in dystrophic muscle (Turner et al., 1988; Mongini et al., 1988; Fong et al., 1990; Williams et al., 1990), which leads to increased muscle protein degradation (Turner et al., 1988; MacLennan et al., 1991). This theory

of increased calcium influx is based on several lines of evidence: (a)  $[\text{Ca}^{2+}]_i$  measurements, which showed higher  $[\text{Ca}^{2+}]_i$  levels near the sarcolemma of stressed dystrophic fibers; (b) calcium transient measurements, which suggest that calcium sequestering mechanisms such as pumps and buffers are unaltered in dystrophic fibers; (c)  $[\text{Na}^+]_i$  measurements demonstrating no sodium permeability increase in dystrophic fibers or myotubes; (d) single-channel studies which showed that leak channels open more frequently in dystrophic myotubes, are voltage-independent, and selectively conduct calcium ions; and (e) studies which showed that pharmacological agents which increased leak channel activity also increased resting  $[\text{Ca}^{2+}]_i$  by significant amounts.

Resting  $[\text{Ca}^{2+}]_i$  levels are elevated by as much as two- to fourfold in dystrophic fibers (Turner et al., 1988; Williams et al., 1990). The results presented here from adult muscle fibers, after increasing  $[\text{Ca}^{2+}]_o$ , support the idea that dystrophic fibers have a reduced ability to regulate free calcium, especially near the sarcolemma (for review see Martonosi, 1989). The higher  $[\text{Ca}^{2+}]_i$  levels near the sarcolemma of *mdx* fibers after  $[\text{Ca}^{2+}]_o$  elevation were not an artifact due to dye compartmentation or reduced dye responsiveness to  $[\text{Ca}^{2+}]_i$  in the fiber interior, since the results from fibers incubated with high  $\text{K}^+$ -Ringer's showed that the dye can respond rapidly throughout the fiber interior. The higher sarcolemmal  $[\text{Ca}^{2+}]_i$  levels were not optical artifacts due to a nonuniform background or low signal intensities at the edge of a fiber, since the  $[\text{Ca}^{2+}]_i$  distribution in prestressed images of fibers was uniform (Fig. 1, b and c). After the stress, the dye signal intensity increased dramatically at 350 nm, and fell slightly at 385 nm (data not shown). Therefore, any edge artifacts would have been more apparent in the prestressed images of fibers.

Actual  $[\text{Ca}^{2+}]_i$  values near the sarcolemma may be higher than estimated here, because of some contribution from the fiber interior to the signal at the edge. Similarly, actual  $[\text{Ca}^{2+}]_i$  values in the fiber center may be lower, because the signal from the center included a contribution from the two edges of the fiber. This would make the actual  $[\text{Ca}^{2+}]_i$  gradients even larger than estimated here.

Intracellular  $[\text{Ca}^{2+}]_i$  gradients of the order of magnitude reported here ( $\sim 20$  nM/ $\mu\text{m}$ ) have been seen in rat pancreatic acinar cells (Kasai and Augustine, 1990), and in smooth muscle cells (Williams et al., 1985). The gradients in normal and *mdx* fibers are most likely a result of a combination of increased calcium entry at the fiber surface, with calcium sequestration in the fiber interior. The amount of total cell calcium therefore will increase, and presumably this increase will be greater in *mdx* fibers (Bertorini et al., 1982). The lack of such clear regional differences in  $[\text{Ca}^{2+}]_i$  in cultured myotubes may be a result of the smaller size and more variable dimensions of cultured myotubes, although DMD and *mdx* myotubes do have a reduced ability to regulate free calcium (Mongini et al., 1988; Fong et al., 1990).

Increased  $[\text{Ca}^{2+}]_i$  levels in dystrophic cells could theoretically result from increased calcium influx and/or reduced calcium efflux. Previously we have shown that calcium transients evoked by electrical depolarization were longer in *mdx* fibers (Turner et al., 1988). This result suggested that calcium sequestering mechanisms in *mdx* fibers were impaired. For example, reduced buffering by parvalbumin could prolong calcium transients (Irving et al., 1989; Simoneau et al.,

1989; Heizmann et al., 1990). However, by presetting resting  $[Ca^{2+}]_i$  levels in normal and dystrophic fibers, we found that it was the resting  $[Ca^{2+}]_i$  level which determined calcium transient decay time. With a lowered  $[Ca^{2+}]_i$ , the ability of *mdx* fibers to sequester released calcium was unimpaired. Since sequestration is a result of the combined activity of sarcoplasmic reticulum  $Ca^{2+}$ -ATPases, buffering of calcium by molecules such as parvalbumin, and calcium efflux across the sarcolemma, this result suggests that, taken together, these mechanisms are not altered in dystrophic muscle. The sarcoplasmic reticulum  $Ca^{2+}$ -ATPase apparently is unaltered in dystrophic muscle (Martonosi, 1989). The activity of the plasma membrane  $Ca^{2+}$ -ATPase cannot be isolated from the other components of efflux in skeletal muscle.

We checked transient peak  $[Ca^{2+}]_i$  levels in normal and *mdx* fibers using both fura-2 and the lower affinity dye fluo-3, and did not find significant differences in peak heights. Transients calculated from fura-2 records in frog skeletal muscle have been shown previously to be consistent with transients calculated using the low-affinity calcium indicator antipyrilazo III (Klein et al., 1988). Despite possible inaccuracies in our calculated absolute peak  $[Ca^{2+}]_i$  values, it is our conclusion from these studies that transient peaks, and presumably calcium release mechanisms, are not different in dystrophic fibers (Martonosi, 1989).

In part, our assumption that calcium efflux mechanisms are unaltered dystrophy is based on the transient decay results. There is no conclusive evidence showing that the sarcoplasmic reticulum  $Ca^{2+}$ -ATPase is affected in dystrophic muscle (Martonosi, 1989). In addition, there are no reports of lower parvalbumin or other calcium buffer concentrations in dystrophic muscle, or for a reduced calcium efflux across the dystrophic sarcolemma.

Increased calcium influx could result from a nonspecific permeability increase of the sarcolemma to small ions. However, we found that resting  $[Na^+]_i$  levels and maximal sodium influx rates in the absence of  $Na^+/K^+$ -ATPase activity were not different in normal and dystrophic muscle fibers and myotubes. Our SBFI values for resting normal and dystrophic  $[Na^+]_i$  of  $\sim 10$  mM are comparable to values obtained using SBFI in other cell types (Harootunian et al., 1989). Our estimate of  $\sim 10$  mM  $[Na^+]_i$  in fibers using  $Na^+$ -selective electrodes is also comparable to previous work with  $Na^+$ -selective electrodes, where normal mouse *soleus* and *gastrocnemius* resting fiber  $[Na^+]_i$  levels were 9.7 and 13 mM, respectively (Fong et al., 1986). The maximal sodium influx rates of  $\sim 1$  mM/min in both normal and dystrophic cells were higher than those found in fibroblasts ( $\sim 0.5$  mM/min, Harootunian et al., 1989), but lower than those in gastric gland cells ( $\sim 3.0$  mM/min, Negulescu et al., 1990). We conclude that there is no increase in the permeability of dystrophic cells to sodium. The defect appears to be specific for calcium ions and is not an increase in general cation permeability as has been suggested (Franco and Lansman, 1990a,b).

Increased calcium entry into dystrophic muscle could be via calcium leak channels, present in the sarcolemma, and perhaps the t-tubule system. Our present estimates of leak channel  $P_o$ , based on longer recording times, show that calcium leak channel activity was again much greater in dystrophic myotubes, in both cell-attached and excised patches.

Channel activity was not significantly altered after patch excision, a finding which suggests that ATP and other intracellular solutes, including calcium, were not responsible for the differences in channel  $P_o$ . Channel openings were voltage independent, and the leak channel was permeable to calcium but not sodium when both ions were present at physiological concentrations. Our hypothesis of increased calcium entry via leak channels in dystrophic cells at rest is based on the assumption that the total number of leak channels is similar in normal and dystrophic cells. Whole cell recording from myotubes could confirm this.

If higher resting  $[Ca^{2+}]_i$  in dystrophic cells is the result of increased leak channel activity, then changes in leak channel activity should result in altered  $[Ca^{2+}]_i$  levels. Leak channel activity was increased by nifedipine. The effect was complex: the mean leak channel  $P_o$  was increased, and channels also entered higher conductance states. The change in  $P_o$  occurred slowly, over a variable time course. We included both early and late records in our calculations of  $P_o$ . Therefore, the average increases we present may underestimate the true response to nifedipine. Multiconductance levels were only seen infrequently with no drugs in the pipette. Similar multiconductance levels have been observed in voltage-gated calcium channels (Kunze and Ritchie, 1990) and in cardiac leak channels (Coulombe et al., 1989). Nifedipine also increased  $[Ca^{2+}]_i$  by significant amounts, a result which supports the idea that leak channel activity can regulate  $[Ca^{2+}]_i$  levels.

Although Bay K 8644 has been shown to increase  $P_o$  in cardiac calcium leak channels (Coulombe et al., 1989), it did not significantly increase myotube leak channel  $P_o$ , or  $[Ca^{2+}]_i$ . We were unable to find any agent which will significantly reduce leak channel activity, but we predict that reduced channel activity will result in lowered  $[Ca^{2+}]_i$ .

Stretch-activated cation leak channels are present in normal mouse myotubes, while there is a prevalence of stretch-inactivated leak channels in *mdx* myotubes (Franco and Lansman, 1990a). We observed small stretch-induced increases in  $[Ca^{2+}]_i$  in normal fibers, but not in *mdx* fibers, where stretch resulted in small drops in  $[Ca^{2+}]_i$ . Our results suggest that although stretch may alter the mechanosensitive leak channel  $P_o$ , the net result in terms of  $[Ca^{2+}]_i$  is not enough to account for the higher *mdx* resting  $[Ca^{2+}]_i$ . The calcium leak channel described here, and the stretch-gated leak channel, are probably different channels. Stretch-gated channels have a higher conductance (18–24 pS with  $Ba^{2+}$ ), and are permeable to sodium and other cations (Franco and Lansman, 1990a,b).

Increased calcium influx might also occur via voltage-gated channels. Differences in the properties of voltage-gated channels have not been reported for dystrophic cells (Trautmann et al., 1986), and the number of voltage-gated calcium channels seems to be unaltered (Desnuelle et al., 1986). We found that various voltage-gated calcium channel blockers, including nifedipine, did not return  $[Ca^{2+}]_i$  in dystrophic fibers or myotubes to normal. Although we did not test the blockers on voltage-gated channels directly, these results suggest that such channels are not a significant pathway for calcium entry into dystrophic myotubes at rest.

How might the lack of dystrophin result in altered leak channel activity? In cystic fibrosis, the absence of a transport receptor protein results in reduced chloride channel activity

(Frizzell et al., 1986; Rich et al., 1990). Analogously, the absence of dystrophin, which is linked to several membrane glycoproteins (Ohlendieck et al., 1991), results in increased leak channel activity. Interactions of the leak channel with cytoskeletal or other proteins might therefore be impaired. The amount of suction required to rupture the sarcolemma in individual patches has been reported to be the same in normal and *mdx* myotubes (Franco and Lansman, 1990a), and our results with SBF1 show that there is no general increase in sarcolemma leakiness or permeability. However, *mdx* myotubes have been shown to be more easily damaged by osmotic shock (Menke and Jockusch, 1991). This result suggests that a lack of dystrophin might alter the physical properties of the sarcolemma, which could affect leak channel gating for example. Further work is needed to help us understand how the absence of dystrophin results in increased calcium leak channel activity.

We would like to thank Dr. Chester M. Regan for help with the ion-selective electrode work and for developing the transient acquisition program; Drs. L. A. Jaffe and A. K. Sater for comments and suggestions on the manuscript; and Dr. R. W. Tsien for helpful discussions.

This work was supported by private donations, the Muscular Dystrophy Association, and the National Institutes of Health.

Received for publication 18 March 1991 and in revised form 4 September 1991.

## References

- Baylor, S. M., and S. Hollingsworth. 1988. Fura-2 calcium transients in frog skeletal muscle fibres. *J. Physiol. (Lond.)*. 403:151-192.
- Bertorini, T. E., S. K. Bhattacharya, G. M. A. Palmieri, C. M. Chesney, D. Pifer, and B. Baker. 1982. Muscle calcium and magnesium content in Duchenne muscular dystrophy. *Neurology*. 32:1088-1092.
- Bulfield, G., W. G. Siller, P. A. L. Wight, and K. J. Moore. 1984. X chromosome-linked muscular dystrophy (*mdx*) in the mouse. *Proc. Natl. Acad. Sci. USA*. 81:1189-1192.
- Campbell, K. P., and S. D. Kahl. 1989. Association of dystrophin and an integral membrane glycoprotein. *Nature (Lond.)*. 338:259-262.
- Coulombe, A., J. A. Lefevre, I. Baro, and E. Coraboeuf. 1989. Barium- and calcium permeable channels open at negative membrane potentials in rat ventricular myocytes. *J. Membr. Biol.* 111:57-67.
- Desnuelli, C., J.-F. Renaud, G. Delpont, G. Serratrice, and M. Lazdunski. 1986. [<sup>3</sup>H]nitrendipine receptors as markers of a class of putative voltage-sensitive Ca<sup>2+</sup> channels in normal human skeletal muscle and in muscle from Duchenne muscular dystrophy patients. *Muscle & Nerve*. 9:148-151.
- Dimario, J., and R. C. Strohman. 1988. Satellite cells from dystrophic (*mdx*) mouse muscles are stimulated by fibroblast growth factor in vitro. *Differentiation*. 39:42-49.
- Duncan, C. J. 1978. Role of intracellular calcium in promoting muscle damage: a strategy for controlling the dystrophic condition. *Experientia (Basel)*. 34:1531-1535.
- Edwards, C. 1982. The selectivity of ion channels in nerve and muscle. *Neuroscience*. 7:1335-1366.
- Fong, C. N., H. L. Atwood, and M. P. Charlton. 1986. Intracellular sodium activity at rest and after tetanic stimulation in muscles of normal and dystrophic (*dy2J/dy2J*) C57BL/6J mice. *Exp. Neurol.* 93:359-368.
- Fong, P., P. R. Turner, W. F. Denetclaw, and R. A. Steinhardt. 1990. Increased activity of calcium leak channels in myotubes of Duchenne human and *mdx* mouse origin. *Science (Wash. DC)*. 250:673-676.
- Franco, A., Jr., and J. B. Lansman. 1990a. Calcium entry through stretch-inactivated ion channels in *mdx* myotubes. *Nature (Lond.)*. 344:670-673.
- Franco, A., Jr., and J. B. Lansman. 1990b. Stretch-sensitive channels in developing muscle cells from a mouse cell line. *J. Physiol. (Lond.)*. 427:361-380.
- Frizzell, R. A., G. Rechkemmer, and R. L. Shoemaker. 1986. Altered regulation of airway epithelial cell chloride channels in cystic fibrosis. *Science (Wash. DC)*. 233:558-560.
- Grynkiewicz, G., M. Poenie, and R. Y. Tsien. 1985. A new generation of Ca<sup>2+</sup> indicators with greatly improved fluorescence properties. *J. Biol. Chem.* 260:3440-3450.
- Hamill, O. P., A. Marty, E. Neher, B. Sakmann, and F. J. Sigworth. 1981. Improved patch clamp techniques for high-resolution current recording from cells and cell-free membrane patches. *Pflügers Arch. Eur. J. Physiol.* 391:85-100.
- Harootyan, A. T., J. P. Kao, B. K. Eckert, and R. Y. Tsien. 1989. Fluorescence ratio imaging of cytosolic free Na<sup>+</sup> in individual fibroblasts and lymphocytes. *J. Biol. Chem.* 264:19458-19467.
- Heizmann, C. W., J. Rohrenbeck, and W. Kamphuis. 1990. Parvalbumin, molecular and functional aspects. *Adv. Exp. Med. Biol.* 269:57-66.
- Hoffman, E. P., R. H. Brown, Jr., and L. M. Kunkel. 1987a. Dystrophin: the protein product of the Duchenne muscular dystrophy locus. *Cell*. 51:919-928.
- Hoffman, E. P., A. P. Monaco, C. C. Feener, and L. M. Kunkel. 1987b. Conservation of the Duchenne muscular dystrophy gene in mice and humans. *Science (Wash. DC)*. 238:347-350.
- Iaizzo, P. A., M. Seewald, S. G. Oakes, and F. Lehmann-Horn. 1989. The use of Fura-2 to estimate myoplasmic [Ca<sup>2+</sup>] in human skeletal muscle. *Cell Calcium*. 10:151-158.
- Irving, M., J. Maylie, N. L. Sizto, and W. K. Chandler. 1989. Simultaneous monitoring of changes in magnesium and calcium concentrations in frog cut twitch fibers containing antipyrilazo III. *J. Gen. Physiol.* 93:585-608.
- Kao, J. P., A. T. Harootyan, and R. Y. Tsien. 1989. Photochemically generated cytosolic calcium pulses and their detection by fluo-3. *J. Biol. Chem.* 264:8179-8184.
- Kasai, H., and G. J. Augustine. 1990. Cytosolic Ca<sup>2+</sup> gradients triggering unidirectional fluid secretion from exocrine pancreas. *Nature (Lond.)*. 348:735-738.
- Klein, M. G., B. J. Simon, G. Szucs, and M. F. Schneider. 1988. Simultaneous recording of calcium transients in skeletal muscle using high- and low-affinity calcium indicators. *Biophys. J.* 53:971-988.
- Kunze, D. L., and A. K. Ritchie. 1990. Multiple conductance levels of the dihydropyridine-sensitive calcium channel in GH<sub>3</sub> cells. *J. Membr. Biol.* 118:171-178.
- MacLennan, P. A., A. McArdle, and R. H. T. Edwards. 1991. Effects of calcium on protein turnover of incubated muscles from *mdx* mice. *Am. J. Physiol.* 260:E594-E598.
- Martonosi, A. 1989. Calcium regulation in muscle diseases; the influence of innervation and activity. *Biochim. Biophys. Acta*. 991:155-242.
- Menke, A., and H. Jockusch. 1991. Decreased osmotic stability of dystrophin-less muscle cells from the *mdx* mouse. *Nature (Lond.)*. 349:69-71.
- Minta, A., and R. Y. Tsien. 1989. Fluorescent indicators for cytosolic sodium. *J. Biol. Chem.* 264:19449-19457.
- Minta, A., J. P. Kao, and R. Y. Tsien. 1989. Fluorescent indicators for cytosolic calcium based on rhodamine and fluorescein chromophores. *J. Biol. Chem.* 264:8171-8178.
- Mongini, T., D. Ghigo, C. Doriguzzi, F. Bussolino, G. Pescarmona, B. Pollo, D. Schiffer, and A. Bosia. 1988. Free cytoplasmic Ca<sup>2+</sup> at rest and after cholinergic stimulus is increased in cultured muscle cells from Duchenne muscular dystrophy patients. *Neurology*. 38:476-480.
- Negulescu, P. A., A. Harootyan, R. Y. Tsien, and T. E. Machen. 1990. Fluorescence measurements of cytosolic free Na concentration, influx and efflux in gastric cells. *Cell Regulation*. 1:259-268.
- Ohlendieck, K., J. M. Ervasti, J. B. Snook, and K. P. Campbell. 1991. Dystrophin-glycoprotein complex is highly enriched in isolated skeletal muscle sarcolemma. *J. Cell Biol.* 112:135-148.
- Poenie, M., J. Alderton, R. Steinhardt, and R. Tsien. 1985. Calcium rises abruptly and briefly throughout the cell at the onset of anaphase. *Science (Wash. DC)*. 223:886-889.
- Rich, D. P., M. P. Anderson, R. J. Gregory, S. H. Cheng, S. Paul, D. M. Jefferson, J. D. McCann, K. W. Klinger, A. E. Smith, M. J. Welsh. 1990. Expression of cystic fibrosis transmembrane conductance regulator corrects defective chloride channel regulation in cystic fibrosis airway epithelial cells. *Nature (Lond.)*. 347:358-363.
- Roe, M. W., J. J. Lemasters, and B. Herman. 1990. Assessment of fura-2 for measurements of cytosolic free calcium. *Cell Calcium*. 11:63-73.
- Simoneau, J. A., M. Kaufmann, K. T. Hartner, and D. Pette. 1989. Relations between chronic stimulation-induced changes in contractile properties and the Ca<sup>2+</sup>-sequestering system of rat and rabbit fast-twitch muscles. *Pflügers Arch. Eur. J. Physiol.* 414:629-633.
- Sugita, H., K. Arahata, T. Ishiguro, Y. Suhara, T. Tsukahara, S. Ishiura, C. Eguchi, I. Nonaka, and E. Ozawa. 1987. Negative immunostaining of Duchenne muscular dystrophy and muscle surface membrane with antibody against synthetic peptide fragment predicted from DMD cDNA. *Proc. Jpn. Acad. Ser. B. Phys. Biol.* 64:37-39.
- Trautmann, A., C. Delaporte, and A. Marty. 1986. Voltage-dependent channels of human muscle cultures. *Pflügers Arch. Eur. J. Physiol.* 406:163-172.
- Tsien, R. Y., and T. J. Rink. 1980. Neutral carrier ion-selective microelectrodes for measurement of intracellular free calcium. *Biochim. Biophys. Acta*. 599:623-638.
- Turner, P. R., L. A. Jaffe, and A. Fein. 1986. Regulation of cortical vesicle exocytosis in sea urchin eggs by inositol 1,4,5-trisphosphate and GTP-binding protein. *J. Cell Biol.* 102:70-76.
- Turner, P. R., T. Westwood, C. M. Regan, and R. A. Steinhardt. 1988. Increased protein degradation results from elevated free calcium levels found in muscle from *mdx* mice. *Nature (Lond.)*. 335:735-738.
- Williams, D. A., K. E. Fogarty, R. Y. Tsien, and F. S. Fay. 1985. Calcium gradients in single smooth muscle cells revealed by the digital imaging microscope using fura-2. *Nature (Lond.)*. 318:558-561.
- Williams, D. A., S. I. Head, A. J. Bakker, and D. G. Stephenson. 1990. Resting calcium concentrations in isolated skeletal muscle fibers of dystrophic mice. *J. Physiol. (Lond.)*. 428:243-256.
- Zubryzcka-Gaarn, E. E., D. E. Bulman, G. Karpati, A. H. M. Burghes, B. Belfall, H. J. Klamut, J. Talbot, R. S. Hodges, P. N. Ray, and R. G. Worton. 1988. The Duchenne muscular dystrophy gene product is localized in sarcolemma of human skeletal muscle. *Nature (Lond.)*. 333:466-469.